Available online at www.sciencedirect.com

ScienceDirect

Procedia Computer Science 138 (2018) 346–353

Procedia Computer Science

www.elsevier.com/locate/procedia

CENTERIS - International Conference on ENTERprise Information Systems / ProjMAN - International Conference on Project MANagement / HCist - International Conference on Health and Social Care Information Systems and Technologies, CENTERIS/ProjMAN/HCist 2018

Deformation monitoring of dam infrastructures via spaceborne MT-InSAR. The case of La Viñuela (Málaga, southern Spain)

Antonio M. Ruiz-Armenteros[a,b,c,*], Milan Lazecky[d], Ivana Hlaváčová[e], Matúš Bakoň[f,g], J. Manuel Delgado[c], Joaquim J. Sousa[h], Francisco Lamas-Fernández[i], Miguel Marchamalo[j], Miguel Caro-Cuenca[k], Juraj Papco[l], and Daniele Perissin[m]

[a]*Dpto. Ingeniería Cartográfica, Geodésica y Fotogrametría, Univ. Jaén, EPSJ, Campus Las Lagunillas s/n, Edif. A3, 23071 Jaén, Spain*
[b]*Centro de Estudios Avanzados en Ciencias de la Tierra CEACTierra, Universidad de Jaén, Spain*
[c]*Grupo de investigación Microgeodesia Jaén, Universidad de Jaén, Spain*
[d]*IT4Innovations, VSB-TU Ostrava, Czech Republic*
[e]*GISAT, s.r.o., Czech Republic*
[f]*University of Presov in Presov, Fac. of Management, Dept. of Environmental Management, Konstantinova 16, 080 01 Presov, Slovak Republic*
[g]*insar.sk s.r.o., Lesna 35, 080 01 Presov, Slovak Republic*
[h]*UTAD, Vila Real and INESC-TEC (formerly INESC Porto), Portugal*
[i]*Departamento de Ingeniería Civil, Universidad de Granada, Granada, Spain*
[j]*Topography and Geomatics Lab. ETSI Caminos, Canales y Puertos, Universidad Politécnica de Madrid, Spain*
[k]*Department of Radar Technology, TNO, The Netherlands*
[l]*Department of Theoretical Geodesy, STU Bratislava, Slovakia*
[m]*Lyles School of Civil Engineering, Purdue University, West Lafayette, IN47907, USA*

Abstract

Dams require continuous security and monitoring programs, integrated with visual inspection and testing in dam surveillance programs. New approaches for dam monitoring focus on multi-sensor integration, taking into account emerging technologies such as GNSS, optic fiber, TLS, InSAR techniques, GBInSAR, GPR, that can be used as complementary data in dam monitoring, eliciting causes of dam deformation that cannot be assessed with traditional techniques. This paper presents a Multi-temporal InSAR (MT-InSAR) monitoring of La Viñuela dam (Málaga, Spain), a 96 m height earth-fill dam built from 1982 to 1989. The presented MT-InSAR monitoring system comprises three C-band radar (~5,7 cm wavelength) datasets from the European satellites ERS-1/2 (1992-2000), Envisat (2003-2008), and Sentinel-1A/B (2014-2018). ERS-1/2 and Envisat datasets were

* Corresponding author. Tel.: +34 953 218 851; fax: +34 953 212 854
E-mail address: amruiz@ujaen.es

Selection and peer-review under responsibility of the scientific committee of the CENTERIS - International Conference on ENTERprise Information Systems / ProjMAN - International Conference on Project MANagement / HCist - International Conference on Health and Social Care Information Systems and Technologies.
10.1016/j.procs.2018.10.049

processed using StaMPS. In the case of Sentinel-1A/B, two different algorithms were applied, SARPROZ and ISCE-SALSIT, allowing the comparison of the estimated LOS velocity pattern. The obtained results confirm that LaViñuela dam is deforming since its construction, as an earth-fill dam. Maximum deformation rates were measured in the initial period (1992-2000), being around -7 mm/yr (LOS direction) on the coronation of the dam. In the period covered by the Envisat dataset (2003-2008), the average deforming pattern was lower, of the order of -4 mm/yr. Sentinel-1A/B monitoring confirms that the deformation is still active in the period 2014-2018 in the central-upper part of the dam, with maximums of velocity reaching -6 mm/yr. SARPROZ and ISCE-SALSIT algorithms provide similar results. It was concluded that MT-InSAR techniques can support the development of new and more effective means of monitoring and analyzing the health of dams complementing actual dam surveillance systems.

Keywords: Dams; La Viñuela; InSAR; Deformation; Sentinel-1; ERS-1/2; Envidat; SAR.

1. Introduction

Monitoring the deformation of large dams is of vital importance for avoiding catastrophic loss of infrastructure and life. Although measuring and monitoring deformations of such man-made structures is a mandatory task, imposed by law worldwide[1] due to the high risk they represent, they usually are time consuming and very expensive, though undeniably very accurate and reliable. Indeed, current dam deformation monitoring schemes rely on the use of dedicated devices, like laser alignment, total station and inverse plummet, occasionally integrated with GNSS for specific monitoring purposes[2-10].

Multi-temporal InSAR (MT-InSAR)[11] evolved to a mature technique and nowadays is successfully applied in measuring of small deformations caused by natural phenomena or in man-made structures. Structural monitoring of dams using MT-InSAR is not yet a widespread application and only a relative few number of studies have been conducted during the past 15 years for structural health monitoring of dams using SAR data[12-24]. However, these achievements allowed to conclude that MT-InSAR techniques have the potential to support the development of new and more effective means of monitoring and analyzing the health of dams and add redundancy, at low cost, to support and assist warning systems. The availability of high quality SAR data is converting MT-InSAR techniques into near-real-time operational tools with the capacity of providing useful information with increased sensitivity to displacements that highlights the dynamic behavior of man-made structures.

In this study, C-band radar data from the European satellites ERS-1/2, Envisat, and Sentinel-1A/B were used to derive mean LOS velocity maps in La Viñuela dam (Spain), a structure oriented in WNW-ESE direction, and the surrounding area. Two independent MT-InSAR tool packages were applied to the dataset covering the period from May 1992 to February 2018. Both approaches confirmed that dam body is prone to deformation.

The paper is structured as follows. Section 2 includes a general description of La Viñuela dam. Section 3 describes the SAR data used in this study as well the processing methodologies carried out. A general description of the deformation results is presented in Section 4 and the main conclusions are derived.

2. La Viñuela dam

The Reservoir of La Viñuela is located on the Guaro River, in the municipality of La Viñuela (province of Málaga, southern Spain) (Fig. 1). It controls the waters of the hydrographic network of the region of La Axarquía and was built to supply drinkable water to the region, to improve the irrigated lands as well as flood lamination. The Guaro River is born in Periana and receives waters from its tributaries, the Sabar, Benamargosa, and Salia Rivers[25,26].

The basin of La Viñuela reservoir has an own surface of 119 km^2, an average yearly rainfall of 893 mm and an average yearly contribution of 25 km^3. The reservoir is made of loose materials (embankment dam), having a coronation length of 460 m, and heights of 96 m over foundations and of 90 m over the riverbed (Fig. 2). It presents a chute spillway with frontal lobe in arch with a pouring length of 30 m and a maximum flow of 382 m^3/s. The bottom drainage consists of a detour tunnel with tow pipes discharging a maximum of 70 m^3/s. The Reservoir of La Viñuela has a surface of 565 ha and a capacity of 170 hm^3. The construction of the dam started on October 22, 1982 and finished in 1989, although it filled completely first in 1998.

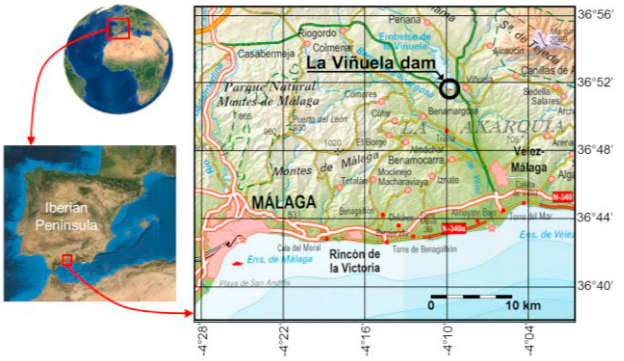

Fig. 1. Location of La Viñuela dam in the province of Málaga.

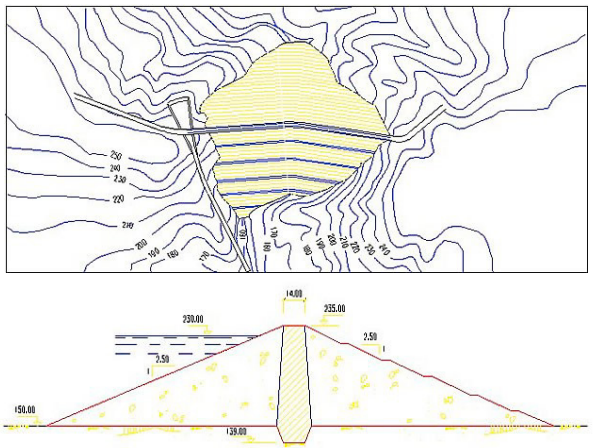

Fig. 2. Plant and cross section of La Viñuela dam. (Source:[25]).

3. Data and Method

3.1. Data

The dam has been analyzed using C-band radar data (~5,7 cm wavelength) from the European satellites ERS-1/2, Envisat, and Sentinel-1A/B. 24 SLC ERS-1/2 SAR images were used, corresponding to descending orbits (track 51) acquired between May 5, 1992 and January 28, 2000 with an incident angle of 23º and a 5x25 m nominal spatial resolution (azimuth x range). Due to ERS-2 on-board gyroscope failure on January 2001, only images until the end of 2000 were selected to avoid high Doppler centroid differences of more than the critical value of 700 Hz. The SLC Envisat ASAR dataset is composed of 27 images acquired from March 21, 2003 to August 1, 2008, along ascending orbits (track 459), with an incidence angle of 23º at the middle swath IS2, and a 5x25 m nominal pixel dimension. The Sentinel-1A/B SAR dataset is formed by 126 SLC IW images (86 Sentinel-1A and 40 Sentinel-1B) acquired in descending orbits from November 16, 2014 to February 28, 2018 with an incidence angle of 37-39º in the center of sub-swath 2 and a pixel spacing of 2.3 x 14.1 m (range x azimuth).

3.2. Multi-Temporal InSAR

DInSAR is limited by temporal and geometrical decorrelation. MT-InSAR methods are helpful to overcome these limitations. The idea behind these methods is to discern coherent radar signal from incoherent contributions in order to obtain only those observations which are physically meaningful. In other words, a PS (Permanent or Persistent Scatterer) is an isolated point with interpretable phase characteristics in time. Methods for identifying and isolating these PS in interferograms have been developed using a functional model to map deformation variation with time. The methods have been very successful in identifying PS pixels in both urban and non-urban areas undergoing primarily steady-state or periodic deformation.

Currently, there are two broad categories of MT-InSAR techniques, persistent scatterer (PSI) methods (e.g.[11,27,28]) and small baseline (SB) methods (e.g.[29,30]). In the following subsections, we briefly describe some characteristics of the used InSAR tool packages.

3.2.1. ERS-1/2 and Envisat processing

The ERS-1/2 and Envisat datasets were processed using StaMPS. This software package developed in MATLAB® implements a PSI method developed to work even in terrains devoid of man-made structures and/or undergoing non-steady deformation[31]. StaMPS-MTI (MT-InSAR) is an extended version of StaMPS that also includes an SB method and a combined MT-InSAR method, allowing the identification of scatterers that dominate the scattering from the resolution cell (PS) and slowly decorrelation-filtered phase (SDFP) pixels, that is, pixels whose phase when filtered decorrelates little over short time intervals[32].

The processing chain begins by reading the SAR scenes and precise orbits. Then, the master scene (December 4, 1998 for the ERS-1/2 dataset and November 5, 2004 in the case of Envisat) is selected in order to start the InSAR processing. Parameters such as the effective baseline, the acquisition date, the Doppler centroid frequency, and the season of the acquisition, form the selection criteria. During the differential interferometric processing steps the observation geometry of the radar acquisition is simulated. A Digital Elevation Model (DEM) and precise orbits are used as input. That means that the interferometric phase can be modeled. The differential interferometric phase is used in all further computations.

StaMPS uses both amplitude and phase analysis to determine the PS probability for individual pixels. First an initial selection based only on amplitude analysis is performed, and then the PS probability is refined using phase analysis in an iterative process. Once selected, the signal due to deformation in the PS pixels is isolated. In contrast to the standard PSI approach[11,28], this PSI method does not require any *a priori* assumptions about the temporal nature of the deformation for PS selection. This is achieved by using the spatially correlated nature of deformation rather than requiring a known temporal dependence. More details about the way that StaMPS identifies PS from interferograms can be found in[33]. The SB method uses amplitude dispersion values and then identifies the SDFP pixels performing phase analysis in space and time. Because PSI and SB approaches are optimized for resolution elements with different scattering characteristics, they are complementary, and techniques that combine both approaches are able to extract the signal with greater coverage than either method alone[32,34]. Thus, both selections (PS + SDPF) are combined and a 3D phase unwrapping algorithm is applied to isolate the deformation signal, based on these pixels. The inner workings of this software package are described in more detail in[27,32,33,35]. In this study, we used the combined processing for both ERS-1/2 and Envisat datasets. The reference area for processing was placed in a stable small urbanization 600 m east to the dam, outside of the dam body.

3.2.2. Sentinel-1A/B processing

The processing of the Sentinel-1A/B dataset was carried out using two different algorithms, SARPROZ and ISCE-SALSIT, allowing the comparison of the estimated LOS velocity patterns. They are briefly described in the following subsections. The reference area for the PS-InSAR processing was selected in the same place as for ERS-1/2 and Envisat processing.

3.2.2.1. SARPROZ

For this case study, the standard PSInSAR analysis (PSI) implemented in SARPROZ software[36] has also been utilized for the purposes of comparison between different methodologies. The processing was performed on a same set of Sentinel-1A/B radar images at a local scale (approx. 1.3 x 0.6 km) allowing for neglecting the atmospheric perturbations as the correlation distance of Atmospheric Phase Screen (APS) is less than few kilometers[37]. Within the standard PSInSAR processing[11], persistent scatterer (PS) candidates were chosen by applying threshold on Amplitude Stability Index. For the selected points, height and displacement were estimated and deformation time series were reconstructed.

3.2.2.2. IT4S1 approach (ISCE-SALSIT)

This area has been processed by an approach recognized as IT4S1[38,39,40]. Here, the Sentinel-1A/B data are specifically preprocessed using the InSAR Scientific Computing Environment (ISCE)[41]. Coregistration process together with the necessary fine corrections and also topography and flat Earth phase removal have been all performed directly to the SLC data. Afterwards, interferometric combinations were prepared for PSI processing using a custom solution, SALSIT[40]. SALSIT (Small Area Least-Squares InSAR Tool) is a new octave-based package, used for standard InSAR processing based on least-squares (LS) method (similar to e.g. StaMPS). It is designed for small objects or small areas, not treating atmospheric effects (however, it can find and exclude images with significantly high level of noise, such as due to snow cover or atmospheric effects). The criteria for point selection are similar to other software, such as StaMPS, amplitude dispersion index (but without PS weeding) with eventual masking.

In comparison to the FFT-based software (such as SARPROZ), for the LS approach it is more difficult to find global minimum of the optimized criteria (minimum standard deviation, i.e. residue RMS, in comparison to the maximum coherence): the iterative process of ambiguity estimation may often aim to a local minima instead of the global one, and there is no way to recognize it. In SALSIT, this is dealt on the basis of quality and closeness of the points, and a point is usually evaluated using more of its neighbors in a PS net (first, the Delaunay net is used, in the second step, new (or old points with low quality) points are connected to several closest points) and evaluated w.r.t. them. However, the LS solution seems to be more sensitive to biased measurements (e.g. due to strong atmospheric effects), the results, with the standard deviation of all the estimated parameters, are familiar to geodesists, who do not understand the coherence, a parameter conventionally used in InSAR community. In addition, the value of standard deviation is necessary to decide whether a PS shall be treated as a moving one, or if the estimated movement velocity is low enough to be taken as noise. Also, the LS approach can be easily adapted to implement other movement models, such as short-term movement, starting movement etc., which seems to be useful for an early-warning approach in future.

4. Results and conclusions

Fig. 3 shows the mean LOS velocity maps derived from StaMPS for ERS-1/2 (May 1992- January 2000) and Envisat (March 2003-August 2008) processing. Both results correspond to the combined (PSI+SB) processing. In the case of ERS-1/2, a deformation pattern can be clearly seen with maximum values around -7 mm/yr on the coronation of the dam. In the Envisat period, the deformation pattern is lower, with maximum values of the order of -4 mm/yr. The standard deviations of the LOS velocity are quite low, of the order of ±1 mm/yr.

The standard PSInSAR approach from SARPROZ with the linear model assumption for the deformation estimates confirmed that the investigated area of the dam body is prone to deformation of up to -6 mm/yr (LOS velocity) in the whole monitoring period of Sentinel-1A/B (November 2014 – February 2018, 126 IW SLC images). The majority of PS points that exhibits deforming motion are also located within the upper part of the dam body (Fig. 4a) as also shown in previous periods. The maximum of velocity there is reaching -6 mm/yr. The same trend for Sentinel-1A/B is shown using ISCE-SALSIT, with mean LOS velocities in the same range (Fig. 4b).

In DInSAR, the movement direction can be estimated only having the measurements from different directions, i.e. ascending and descending passes (from the same time period). And even in such cases, it is difficult to detect the movements in the north-south direction, as the sensitivity of the LOS direction to this direction is lower than 0.1. The possibility to detect the horizontal (east-west) movements depends on the satellite incidence angle, making it higher for Sentinel-1A/B than for ERS-1/2/Envisat tracks. The movement of the dam is expected only in the vertical and cross-dam directions (the direction perpendicular to the dam body). Here, the dam body is almost parallel to the LOS direction (in the horizontal plane), causing very low sensitivity (0.03-0.06) of the detection of the cross-dam movements, for all descending tracks (ERS-1/2 and Sentinel-1A/B). Therefore, if the along-dam movements can be neglected, all the measured LOS movement can be attributed to subsidence. For Envisat, the sensitivity of the cross-dam movements is 0.17, in comparison to 0.92 for the vertical direction. The rate of the figures represents how the

vertical and cross-dam components contribute to the LOS movement. Therefore, if the cross-dam component is 5-times higher than the vertical one, their contribution to the LOS movement is comparable.

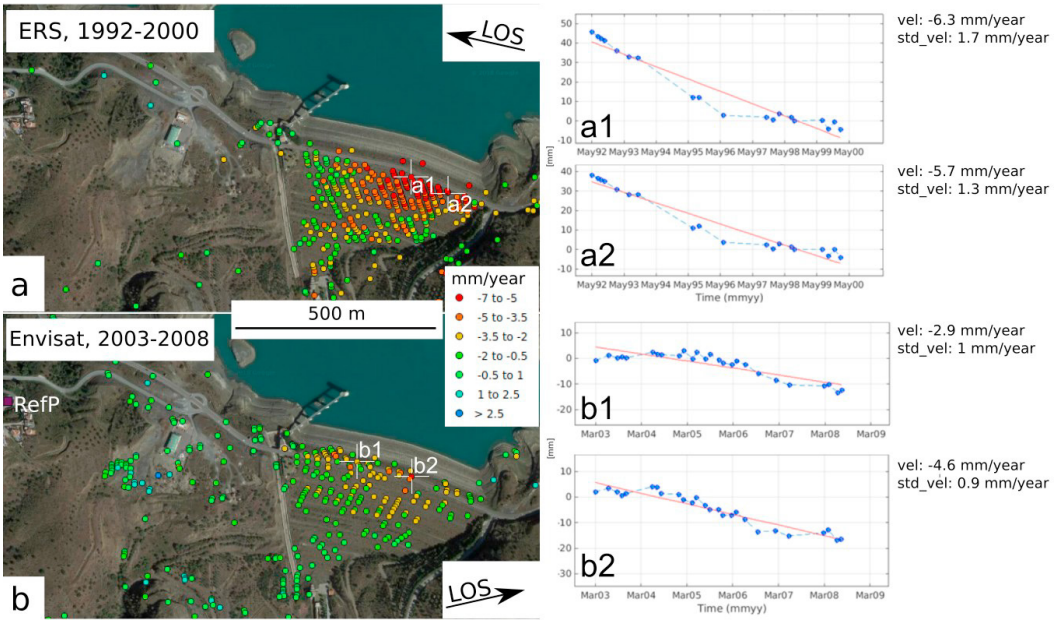

Fig. 3. Mean LOS velocity and its standard deviation for ERS-1/2 (1992-2000) (a) and Envisat (2003-2008) (b) processing. Two time-series representative of the deformation are plotted for each processing.

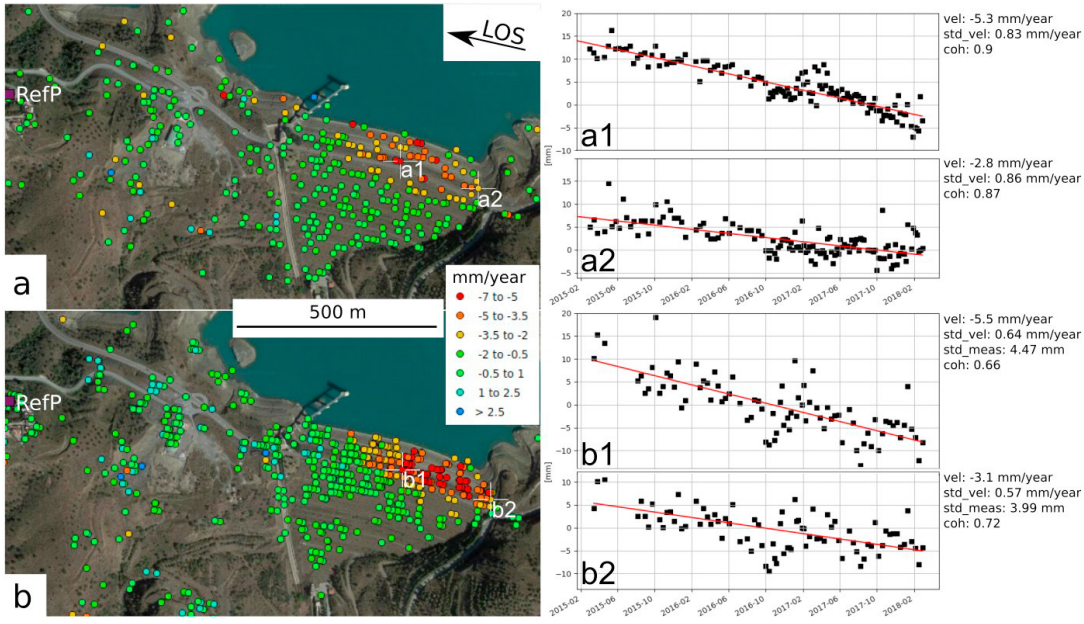

Fig. 4. Mean LOS velocity for Sentinel-1A/B (2014-2018) processing using SARPROZ (a) and ISCE-SALSIT (b). Two time-series representative of the deformation are plotted for each processing.

It is not reliable to compare two datasets from different time periods, but the velocities measured by Envisat are significantly lower than those measured by ERS-1/2. This can be attributed either to the stabilization of the dam in

time, and also to the contribution of the (significant) cross-dam movement. In addition, in the upper part of the dam, the Sentinel-1A/B measured velocities are higher again, confirming the significant cross-dam movement. The cross-dam movement is expected to correlate with water level, while the vertical movement is expected to stabilize in time.

This study shows the potential of C-band SAR data for monitoring deformation of one earth-fill dam. The ratio of the detected deformation might be assumable for this kind of dams. Future investigations will address a mathematical modeling of the dam to investigate the expected theoretical deforming behavior due to the material consolidation through time. Additionally, some other geotechnical/geodetic data, if available, could be used to validate the MT-InSAR deformation pattern.

Acknowledgements

ERS-1/2 and Envisat data were provided by the European Space Agency (ESA) in the scope of 28654 G-POD and 7629 CAT-1 projects. Sentinel-1A/B data were freely provided by ESA through Copernicus Programme. Data have been processed by DORIS from TUDelft, StaMPS, SARPROZ (Copyright (c) 2009-2018 Daniele Perissin), ISCE from NASA/JPL and G-POD service of ESA. The satellite orbits are from Delft University of Technology and ESA, as well as from the ESA Quality control Group of Sentinel-1. Research was supported by: (a) ESA Research and Service Support for providing hardware resources employed in this work, (b) ReMoDams project ESP2017-89344-R (AEI/FEDER, UE) from Spanish Ministry of Economy, Industry and Competitiveness, PAIUJA-2017/2018 and CEACTierra from University of Jaén (Spain), and RNM-282 research group from the Junta de Andalucía (Spain), (c) ERDF through the Operational Programme for Competitiveness and Internationalisation - COMPETE 2020 Programme within project «POCI-01-0145-FEDER-006961», and by National Funds through the FCT – Fundação para a Ciência e a Tecnologia (Portuguese Foundation for Science and Technology) as part of project UID/EEA/50014/2013, (d) The Ministry of Education, Youth and Sports from the National Programme of Sustainability (NPU II) project «IT4Innovations excellence in science - LQ1602» (Czech Republic). Large Infrastructures for Research, Experimental Development and Innovations project „IT4Innovations National Supercomputing Center – LM2015070“, and (e) Slovak Grant Agency VEGA under projects No. 1/0714/15 and 1/0462/16.

References

[1] ICOLD (2012) “Dam surveillance guide. Guide de la surveillance des barrages”. Bulletin 158. 109 pp (available online at http://www.icold-cigb.net/GB/publications/publications.asp, last accessed: April 28th, 2018).

[2] Chouinard, L.E., Bennett, D.W., and Feknous, N. (1995) “Statistical analysis of monitoring data for concrete arch dams”. *Journal of Performance of Constructed Facilities* **9**(**4**): 286–301.

[3] Behr, J., Hudnut, K., and King, N., (1998) “Monitoring structural deformation at Pacoima dam, California using continuous GPS”. *Proceedings of ION GPS* l, 11: 59–68, Institute of Navigation.

[4] De Sortis, A., and Paoliani, P. (2007) “Statistical analysis and structural identification in concrete dam monitoring”. *Engineering Structures* **29**(**1**): 110–120.

[5] Lombardi, G., Amberg, F., and Darbre, G.R. (2008) “Algorithm for the prediction of functional delays in the behaviour of concrete dams”. *International Journal on Hydropower Dams* **15**(**3**), 111.

[6] Amberg, F. (2009) “Interpretative models for concrete dam displacements” in *Comisión Internacional de Grandes Presas-Vigésimo tercer congreso de Grandes Presas*, Brasilia.

[7] Ehiorobo, J.O., and Irughe-Ehigiator, R. (2011) “Monitoring for horizontal movement in an earth dam using differential GPS”. *Journal of Emerging Trends in Engineering and Applied Sciences* **2**(**6**): 908–913.

[8] Li, W., and Wang, C. (2011) “GPS in the tailings dam deformation monitoring”. *Procedia Engineering* **26**: 1648–1657.

[9] Barzaghi, R., Pinto, L., and Monaci, R. (2012) “The monitoring of gravity dams: two tests in Sardinia, Italy”. *FIG Working Week* (Session TS01F), Rome, Italy, 6–10.

[10] Galán-Martín, D., Marchamalo-Sacristán, M., Martínez-Marín, R., and Sánchez-Sobrino, J.A. (2013) “Geomatics applied to dam safety DGPS real time monitoring”. *International Journal of Civil Engineering* **11**(**2A**): 134-141.

[11] A. Ferretti, C. Prati, and F. Rocca. (2001) “Permanent Scatterers in SAR Interferometry”. *IEEE Transactions on Geoscience and Remote Sensing* **39**(**1**): 8–20.

[12] Tarchi, D., Rudolf, H., Luzi, G., Chiarantini, L., Coppo, P., and Sieber, A.J. (1999) “SAR interferometry for structural changes detection: a demonstration test on a dam”. *Proceedings of the IEEE International Geoscience and Remote Sensing Symposium (IGARSS ‘99),* July, Hamburg, Germany, vol. 3: 1522–1524.

[13] Blom, R., Fielding, E., Gabriel, A., and Goldstein, R. (1999) “Radar interferometry for monitoring of oil fields and dams: Lost Hills, California and Aswan, Egypt”. Issue Date: 25-Oct-1999. *National Geological Society of America Meeting*. Denver, CO, USA.

[14] Wang, T., Perissin, D., Rocca, F., and Liao, M.S. (2010) “Three Gorges Dam stability monitoring with time-series InSAR image analysis”. *Science China Earth Sciences*, **54**(**5**): 720-732. http://dx.doi.org/10.1007/s11430-010-4101-1.

[15] Arjona, A., Santoyo, M.A., Fernández, J., Monells, D., Prieto, J.F., Pallero, J.L.G., Prieto, E., Seco, A., Luzón, F., and Mallorquí, J. (2010) "On the applicability of an advanced DInSAR technique near Itoiz and Yesa reservoirs, Navarra, Spain". *Proceeding of Fringe 2009*. Frascati: ESRI (ESA, SP-677, 1609-042X, 6 pp., CD).

[16] Grenerczy, G., and Wegmüller, U. (2011) "Persistent scatterer interferometry analysis of the embankment failure of a red mud reservoir using ENVISAT ASAR data". *Natural Hazards* **59**: 1047–1053.

[17] Vöge, M., Larsen, Y., and Frauenfelder, R. (2011) "Monitoring dams and reservoir slopes with interferometric SAR". *Proceedings of 8th International Symposium on Field Measurements in GeoMechanics*, Berlin, Germany, September, 12–16.

[18] Tomás, R., Cano, M., Garcia-Barba, J., Vicente, F., Herrera, G., Lopez-Sanchez, J.M., and Mallorquí, J. (2013) "Monitoring an earthfill dam using differential SAR interferometry: La Pedrera Dam, Alicante, Spain". *Engineering Geology* **157**: 21-32.

[19] Di Martire, D., Iglesias, R., Monells, D., Centolanza, G., Sica, S., Ramondini, M., and Calcaterra, D. (2014) "Comparison between differential SAR interferometry and ground measurements data in the displacement monitoring of the earth-dam of Conza della Campania (Italy)". *Remote Sensensing of Environment* **148**: 58–69.

[20] Michoud, C., Baumann, V., Derron, M.H., Jaboyedoff, M., and Lauknes, T.R. (2015) "Slope instability detection along the national 7 and the potrerillos dam reservoir, Argentina, using the small-baseline InSAR technique". *Engineering Geology for Society and Territory*, vol 2. Springer International Publishing, 295–299.

[21] Michoud, C., Baumann, V., Lauknes, T.R., Penna, I., Derron, M.H., and Jaboyedoff, M. (2016) "Large slope deformations detection and monitoring along shores of the Potrerillos dam reservoir, Argentina, based on a small-baseline InSAR approach". *Landslides* **13**(**3**): 451-465.

[22] Sousa, J.J., Lazecky, M., Hlavacova, I., Bakon, M., Patricio, G., and Perissin, D. (2015) "Satellite SAR interferometry for monitoring dam deformations in Portugal". Second International Dam World Conference, Portugal, April 21–24, p. 2015.

[23] Roque, D., Perissin, D., Falcão, A.P., Fonseca, A.M., Henriques, M.J., and Franco, J. (2015) "Dams regional safety warning using time-series InSAR techniques". Second International Dam World Conference, Portugal, April, pp. 21–24.

[24] Mazzanti, P., Perissin, D., and Rocca, A. (2015) "Structural health monitoring of dams by advanced satellite SAR interferometry: investigation of past processes and future monitoring perspectives". 7th International Conference on Structural Health Monitoring of Intelligent Infrastructure, Torino, Italy, July 1–3 2015.

[25] Andalucía Rústica (2018). http://andaluciarustica.com/en/presa_la_vinuela.htm (last accessed: April 28th, 2018)

[26] Embalse de La Viñuela. (n.d.). In Wikipedia. Retrieved April 26, 2018, from http://en.wikipedia.org/wiki/Embalse_de_La_Viñuela (last accessed: April 28th, 2018)

[27] Hooper A, Zebker H, Segall P, and Kampes B. (2004) "A new method for measuring deformation on volcanoes and other natural terrains using InSAR persistent scatterers". *Geophysical Research Letters* **31**: L23611. http://dx.doi.org/10.1029/2004GL021737.

[28] Kampes BM. (2006) "Radar Interferometry: Persistent Scatterer Technique", Kluwer Academic Publishers, Dordrecht, The Netherlands.

[29] Berardino, P., Fornaro, G., Lanari, R., and Sansosti, E. (2002) "A new algorithm for surface deformation monitoring based on small baseline differ-ential SAR interferograms". *IEEE Transactions on Geoscience and Remote Sensing* **40**(**11**), 2375 – 2383.

[30] Schmidt, DA, and Bürgmann, R. (2003) "Time-dependent land uplift and subsidence in the Santa Clara valley, California, from a large interferometric synthetic aperture radar data set". *Journal of Geophysical Research* **108**,**B9**: 2416–2428.

[31] Hooper, A, Bekaert, DPS, Spaans, K, and Arikan M. (2012) "Recent advances in SAR interferometry time series analysis for measuring crustal deformation". *Tectonophysics* **514-517**:1-13. http://dx.doi.org/10.1016/j.tecto.2011.10.013.

[32] Hooper, A. (2008) "A multi-temporal InSAR method incorporating both persistent scatterer and small baseline approaches" *Geophysical Research Letters* **35**:L16302. http://dx.doi.org/10.1029/2008GL034654.

[33] Hooper A, Segall P, and Zebker H. (2007) "Persistent Scatterer InSAR for Crustal Deformation Analysis, with Application to Volcán Alcedo, Galapagos" *Journal of Gephysical Research* **112**, B07407, http://dx.doi.org/10.1029/2006JB004763.

[34] Ferretti, A, Fumagalli, A, Novali, F, Prati, C, Rocca, F, Rucci, A. (2011) "A new algorithm for processing interferometric data-stacks: SqueeSAR" *IEEE Transactions on Geoscience and Remote Sensing* **49**: 3460-3470.

[35] Hooper, A. (2010) "A statistical-cost approach to unwrapping the phase of InSAR time series". European Space Agency (Special Publication) ESA SP-677.

[36] Perissin, D. (2015) "SARPROZ software". Official Product Web page: http://www.sarproz.com

[37] Hanssen, R. (2001) "Radar interferometry, data interpretation and error analysis". Kluwer Academic Publishers

[38] Lazecky, M. (2017) "System for Automatized Sentinel-1 Interferometric Monitoring", 4 pp., Proc. of ESA Big Data in Space 2017, Toulouse, 28-30 Nov 2017, P. Soille and P.G. Marchetti (Eds.), Proceedings of the 2017 conference on Big Data from Space. BIDS' 2017, EUR 28783 EN, Publications Office of the European Union, Luxembourg, 2017, ISBN 978-92-79-73527-1, http://dx.doi.org/10.2760/383579, JRC108361

[39] Lazecky, M. (2018) "Identification of active slope motion in Czech environment using Sentinel-1 interferometry", In: GIS Ostrava 2018, 21-23 Mar 2018, Springer Lecture Notes in Geoinformation and Cartography, 7 p.

[40] Lazecky, M., Hlavacova, I., Martinovič, J., Ruiz-Armenteros, A.M. (2018) "Accuracy of Sentinel-1 Interferometry Monitoring System based on Topography-free Phase Images", In: Workshop SARWatch - Advances in the Science and Applications of SAR Interferometry, CENTERIS - Conference on ENTERprise Information Systems 2018, Lisbon, 21-23 Nov 2018.

[41] Rosen, P., Gurrola, E., Agram, P. S., Sacco, G. F. and Lavalle, M. (2015) "InSAR Scientific Computing Environment (ISCE): A Python Framework for Earth Science", AGU Fall Meeting 2015.